



OPEN ACCESS

EDITED BY

Guangwei Du,
Penn State Milton S. Hershey Medical Center,
United States

REVIEWED BY

Donato Melchionda,
Azienda Ospedaliero-Universitaria Ospedali
Riuniti di Foggia, Italy
Jonathon Maffie,
Penn State Milton S. Hershey Medical Center,
United States

*CORRESPONDENCE

Matteo Paoletti
✉ matteo.paoletti@mondino.it

†These authors share first authorship

RECEIVED 02 January 2025

ACCEPTED 14 April 2025

PUBLISHED 16 May 2025

CITATION

Nicolosi S, Todisco M, Paoletti M,
Caverzasi E, Tarantino F, Ballante E,
Valentino F, Zangaglia R, Figini S,
Cosentino G, Pacchetti C and Pichiecchio A
(2025) Radiological features of gait
phenotypes in patients with idiopathic
normal pressure hydrocephalus.
Front. Aging Neurosci. 17:1554642.
doi: 10.3389/fnagi.2025.1554642

COPYRIGHT

© 2025 Nicolosi, Todisco, Paoletti, Caverzasi,
Tarantino, Ballante, Valentino, Zangaglia,
Figini, Cosentino, Pacchetti and Pichiecchio.
This is an open-access article distributed
under the terms of the [Creative Commons
Attribution License \(CC BY\)](https://creativecommons.org/licenses/by/4.0/). The use,
distribution or reproduction in other forums
is permitted, provided the original author(s)
and the copyright owner(s) are credited and
that the original publication in this journal is
cited, in accordance with accepted academic
practice. No use, distribution or reproduction
is permitted which does not comply with
these terms.

Radiological features of gait phenotypes in patients with idiopathic normal pressure hydrocephalus

Silvia Nicolosi^{1,2†}, Massimiliano Todisco^{3,4†}, Matteo Paoletti^{1*},
Eduardo Caverzasi^{1,5}, Francesco Tarantino⁶, Elena Ballante⁷,
Francesca Valentino⁴, Roberta Zangaglia⁴, Silvia Figini^{7,8},
Giuseppe Cosentino^{3,5}, Claudio Pacchetti⁴ and
Anna Pichiecchio^{1,5}

¹Department of Neuroradiology, Advanced Imaging Center and Artificial Intelligence, IRCCS Mondino Foundation, Pavia, Italy, ²Radiology Section, Department of Clinical-Surgical, Diagnostic, and Pediatric Sciences, University of Pavia, Pavia, Italy, ³Translational Neurophysiology Research Unit, IRCCS Mondino Foundation, Pavia, Italy, ⁴Movement Disorders Research Center, IRCCS Mondino Foundation, Pavia, Italy, ⁵Department of Brain and Behavioral Sciences, University of Pavia, Pavia, Italy, ⁶Department of Radiology, Di Summa-Perrino Hospital Center, Brindisi, Italy, ⁷BioData Science Center, IRCCS Mondino Foundation, Pavia, Italy, ⁸Department of Political and Social Sciences, University of Pavia, Pavia, Italy

Introduction: According to the higher-level gait disorder (HLGD) pattern, patients with idiopathic normal pressure hydrocephalus (iNPH) can be divided into two motor phenotypes; a disequilibrium (wide-based gait) subtype and a parkinsonian (locomotor) subtype. We aimed to understand the neuroimaging correlates of iNPH phenotyping into different gait patterns, by assessing specific radiological features and their correlations with clinical scores.

Methods: We enrolled 86 probable iNPH patients (53 males; age range: 69–88 years), who underwent a comprehensive clinical assessment, including neuropsychological tests, and a conventional MRI scan. The cohort was subdivided into disequilibrium subtype (29 subjects) and parkinsonian subtype of HLGD (57 patients) based on gait evaluation. We compared the iNPH subtypes assessing differences in eight linear radiological indexes and their clinical correlates.

Results: The Height of the third ventricle was the only radiological feature that differed between the two motor phenotypes ($p < 0.05$), being higher in the parkinsonian subtype and showing a trend of correlation with the motor score of the Movement Disorder Society-Unified Parkinson's Disease Rating Scale and with the continence score of the iNPH Rating Scale. Among several clinical-radiological correlations, a reduced callosal angle correlated with the severity of motor and urinary symptoms ($p < 0.05$).

Discussion: A greater height of the third ventricle possibly leading to a top-down compressive effect on the midbrain could be a neuroimaging marker of the parkinsonian phenotype of iNPH. The extensive correlations between linear radiological indices and clinical scales suggest a potential role for radiological features in clinical monitoring.

KEYWORDS

idiopathic normal pressure hydrocephalus, magnetic resonance imaging, gait disorder, parkinsonism, third ventricle

1 Introduction

Idiopathic normal pressure hydrocephalus (iNPH) is a complex cerebrospinal fluid dynamic disorder, clinically characterized by progressive motor, cognitive, and urinary disturbances due to ventricular enlargement, without any significant intracranial pressure abnormalities (Nakajima et al., 2021; Relkin et al., 2005). Despite representing one of the major neurological conditions that can benefit from surgical treatment (Nakajima et al., 2021; Todisco et al., 2020), iNPH is frequently underdiagnosed because subjects may have atypical clinical presentations beyond the classic triad of gait disorder, cognitive decline, and urinary incontinence (Todisco et al., 2019; Todisco et al., 2022).

The higher-level gait disorder (HLGD) represents the core clinical finding in iNPH (94–100% of cases), followed by cognitive impairment (78–98%) and urinary urgency (60–92%) (Relkin et al., 2005). However, gait disturbance of iNPH shows high variability of phenomenology. Indeed, if on the one hand the typical gait pattern is characterized by wide base with externally rotated feet and impaired balance with falls, on the other hand about two-thirds of patients can present parkinsonian features, i.e., slowness, shuffling steps, freezing of gait, and *en bloc* turning (Todisco et al., 2021; Pozzi et al., 2021). This evidence led to the dichotomous classification into a disequilibrium (wide-based gait) subtype, defined as phenotype 1, and a parkinsonian subtype, known as phenotype 2, respectively (Todisco et al., 2021; Pozzi et al., 2021; Nutt, 2013).

Brain magnetic resonance imaging (MRI) plays an essential role in the diagnosis of iNPH, since it provides routinely used radiological indexes—as Evans' Index (EI) and callosal angle (CA) at the level of the posterior commissure—and also assists in patient stratification into the diagnostic categories of “possible” or “probable” iNPH according to the Japanese Guidelines, based on the evaluation of Disproportionately Enlarged Subarachnoid Space Hydrocephalus (DESH) (Nakajima et al., 2021; Relkin et al., 2005). To date, radiological underpinnings of the clinical symptoms in iNPH are still matter of debate. Neuroimaging correlates of the distinct phenotypes of HLGD have not yet been investigated. In this study, we aimed to apply several radiological indexes used for diagnostic and research purposes to assess differences between the two motor phenotypes of iNPH. Moreover, we explored potential correlations of MRI features with clinical severity scores.

2 Materials and methods

2.1 Study subjects

As part of a prospective longitudinal evaluation, between January 2016 and December 2018 we consecutively recruited 86 patients diagnosed as “probable” iNPH according to the International Guidelines and admitted to the Parkinson's Disease and Movement Disorders Unit of the Mondino Foundation in Pavia (Italy) (Nakajima et al., 2021). All subjects were clinically assessed by a movement disorder specialist, who qualitatively established the motor phenotype based on the HLGD pattern as previously detailed (Todisco et al., 2021; Pozzi et al., 2021). No patient was under diuretic treatment. A second blinded

clinician reevaluated the gait subtype of iNPH patients, showing a full agreement. The clinical and neuropsychological evaluation included the iNPH Rating Scale (iNPHRS) (Hellström et al., 2012), the motor section of the Movement Disorder Society-Unified Parkinson's Disease Rating Scale (MDS-UPDRS III) (Goetz et al., 2008) and the education-adjusted scores of the Mini Mental State Examination and of the Montreal Cognitive Assessment (MoCA).

Within six months from the neurological assessment, all patients underwent a 1.5 or 3 Tesla brain MRI scan, including routine sequences for the diagnostic work-up, such as axial fluid-attenuated inversion recovery (FLAIR), coronal and sagittal T2-weighted turbo spin-echo (TSE), and T1-weighted gradient echo (GRE) three-dimensional sequences with multiplanar reconstructions, at the Neuroradiology Unit of the same hospital.

The Ethics Committee of the Mondino Foundation approved the study. All patients gave written informed consent to all study procedures and to personal data processing for research purposes, according to the Declaration of Helsinki. The study protocol was entirely performed before eventual shunt surgery treatment.

2.2 Neuroimaging measurements

Blinded to patients' clinical examination, an expert neuroradiologist (with ten years of experience in the field) reviewed all brain MRI scans, assessing eight quantitative linear radiological indexes, so as to remove the inter-rater variability. The radiological indexes included: EI (Figure 1A); CA (Figure 1B); DESH (Figure 1C); Magnetic Resonance Hydrocephalic Index (MRHI) (Figure 1D); Anteroposterior diameter of the Lateral Ventricle Index (ALVI) (Figure 1E); modified Cella Media Index (mCMI) (Figure 1F); and Height and Width of the third ventricle (IIIvH and IIIvLL, respectively) (Figures 1G, H). EI is the ratio between the maximal width of the frontal horns and the largest internal diameter of the cranium at the same slice. An EI greater than 0.30 is widely used to determine an enlargement of the supratentorial ventricular system (Nakajima et al., 2021; Relkin et al., 2005). CA is measured on the coronal plane through the posterior commissure perpendicular to the anterior-commissural line (AC-PC line). A CA value lower than 90–100° is considered highly accurate to discriminate iNPH patients from healthy controls or patients with Alzheimer's disease, as lower values were found in iNPH (Ishii et al., 2008). DESH is considered present in case of narrowing of the high-convexity and medial subarachnoid spaces with enlarged Sylvian fissures on T1-weighted coronal images (Relkin et al., 2005). MRHI is obtained by dividing the collateral trigones width by the internal diameter of the cranial theca, as previously proposed by Quattrone et al. (2020). ALVI is calculated as the ratio between the width from the most anterior to the most posterior points of the lateral ventricles and the sagittal diameter of the internal cranial theca at the same level (He et al., 2020). mCMI is defined as the ratio between the maximal width of the cella media and the maximal inner diameter of the skull at the same level on an axial plane (Kojoukhova et al., 2015). Both ALVI and mCMI were assessed for each side separately (right and left, i.e., ALVI R/L and mCMI R/L). IIIvH and IIIvLL are calculated as the diameter from the roof to the floor of the third ventricle perpendicular to the AC-PC line and as the greatest

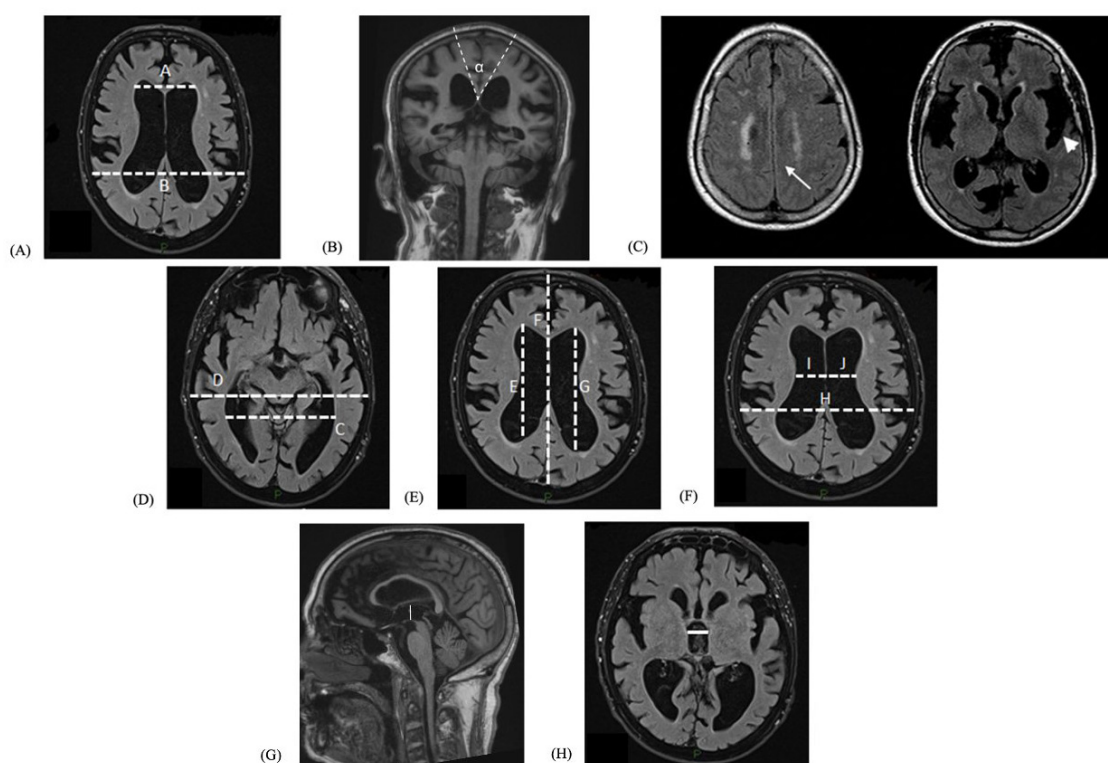


FIGURE 1

Linear radiological indexes. **(A)** Evans' Index: maximal width of the frontal horns (A) and the largest internal diameter of the cranium at the same slice (B). **(B)** Callosal angle: the angle is calculated at the level of posterior commissure (α). **(C)** Disproportionately Enlarged Subarachnoid Space Hydrocephalus: narrowing of the subarachnoid spaces near the vertex (arrow) and widening of the Sylvian fissures (arrowhead). The hyperintense periventricular white matter abnormalities in both axial FLAIR sequences are referred to slight chronic microvascular damage. **(D)** Magnetic Resonance Hydrocephalic Index: the largest left-to-right width of the collateral trigones of the lateral ventricles (C) and maximum inner skull diameter (D). **(E)** Anteroposterior diameter of the Lateral Ventricle Index, evaluated for each side: anteroposterior diameter of each lateral ventricle (E and G, right and left, respectively) and the maximal width of the anteroposterior inner diameter of the skull (along the cerebral falx) (F). **(F)** Modified Cella Media Index, assessed for both sides: the largest internal diameter of the cranium (H) and the maximum cella media width of each lateral ventricle (I and J, right and left, respectively). **(G)** Height of the third ventricle. **(H)** Width of the third ventricle.

latero-lateral diameter of the third ventricle perpendicular to the median line, respectively (Reinard et al., 2015). By means of ruler and angle measurement available on the routine neuroimaging viewing system, the radiological measures were manually taken in the axial plane, except for the CA, calculated on a paracoronal plane perpendicular to the AC-PC line, and the IIIvH, evaluated on sagittal sequences (Reinard et al., 2015).

2.3 Statistical analysis

Statistical analysis was performed using R software version 4.4.2. The Wilcoxon test was used to explore any difference between two motor phenotypes of HLGD, except for the binary categorical variables gender and DESH for which Pearson's chi-squared test with Yates' continuity correction was applied. Considering the small sample size and the high number of correlations, a multiple comparison correction was not applied. For each correlation, the Cohen's *d* effect size was calculated to measure the strength of the relationship between variables and reported in conjunction with *p*-values. The magnitude of the effect size should be assessed using the thresholds provided in Cohen, 1992, i.e., $|d| < 0.2$ "negligible," $|d| < 0.5$ "small," $|d| < 0.8$ "medium," otherwise "large."

Comparisons between radiological indices and clinical scores were calculated using Spearman's rank correlation test, already a measure of the effect, whereas for DESH the Wilcoxon test with continuity correction and relative Cohen's *D* effect size were used. Statistical significance was defined for *p*-values below 0.05.

3 Results

3.1 Demographics, clinical scores and MRI indexes

Demographic, clinical and radiological data for the entire cohort and for each motor phenotype of HLGD are reported in Table 1. Within the whole cohort of 86 iNPH patients, we identified 29 subjects (34%) with phenotype 1 (disequilibrium subtype) and 57 subjects (66%) with phenotype 2 (parkinsonian subtype). The two motor phenotypes did not differ significantly in demographic variables. Conversely, patients with phenotype 2 showed more severe parkinsonism (higher MDS-UPDRS III score), more impaired gait and balance (lower iNPHRS scores at the

TABLE 1 Demographics, clinical data and MRI features of iNPH patients.

	Entire cohort (n = 86)	Phenotype 1 (n = 29)	Phenotype 2 (n = 57)	Effect size	P-values
Age (years)	75 ± 3	76 ± 5	76 ± 6	0.091	0.392
Age at motor symptoms onset (years)	73 ± 6	73 ± 6	73 ± 7	0.028	0.833
Gender (M/F)	53/33	18/11	35/22	0	1
MDS-UPDRS III	19 ± 13	8 ± 4	25 ± 12	1.682	< 0.001
iNPHRS gait	42 ± 23	54 ± 22	36 ± 22	0.798	< 0.001
iNPHRS balance	58 ± 17	65 ± 14	55 ± 17	0.644	0.002
iNPHRS continence	66 ± 23	72 ± 25	62 ± 21	0.458	0.051
iNPHRS total	48 ± 17	57 ± 16	44 ± 15	0.868	< 0.001
MMSE	23 ± 6	25 ± 4	22 ± 7	0.549	0.035
MoCA	17 ± 6	20 ± 6	16 ± 6	0.678	0.015
EI	0.35 ± 0.04	0.35 ± 0.03	0.36 ± 0.04	0.160	0.967
CA (°)	84.39 ± 18.04	89.20 ± 23.03	81.70 ± 18.33	0.374	0.225
DESH (%)	80	81	79	0	1
MRHI	0.57 ± 0.03	0.58 ± 0.04	0.58 ± 0.03	0.109	0.559
ALVI R	0.52 ± 0.04	0.53 ± 0.04	0.54 ± 0.05	0.314	0.466
ALVI L	0.53 ± 0.04	0.54 ± 0.05	0.55 ± 0.05	0.173	0.690
mCMI R	0.16 ± 0.02	0.17 ± 0.02	0.17 ± 0.02	0.183	0.315
mCMI L	0.16 ± 0.03	0.18 ± 0.02	0.17 ± 0.03	0.397	0.065
IIIvH	13.99 ± 1.65	13.40 ± 1.55	14.3 ± 1.62	0.593	0.017
IIIvLL	13.36 ± 2.81	13.60 ± 2.70	13.20 ± 2.88	0.132	0.304

Findings from the entire cohort and from each motor phenotype, expressed as mean ± standard deviation or as numbers or percentages. Statistical *p*-values and Cohen's *d* effect sizes of comparisons between the two motor phenotypes are reported. Statistically significance values are in bold. ALVI, Anteroposterior diameter of the Lateral Ventricle Index; CA, callosal angle; DESH, Disproportionately Enlarged Subarachnoid Space Hydrocephalus; EI, Evans' Index; iNPH, idiopathic normal pressure hydrocephalus; iNPHRS, iNPH Rating Scale; L, left; mCMI, modified Cella Media Index; MDS-UPDRS III, motor score of the Movement Disorder Society-Unified Parkinson's Disease Rating Scale; MMSE, Mini Mental State Examination; MoCA, Montreal Cognitive Assessment; MRHI, Magnetic Resonance Hydrocephalic Index; R, right; IIIvH, height of the third ventricle; IIIvLL, width of the third ventricle.

related items), worse cognitive scores (lower MMSE and MoCA scores), and poorer global functioning (lower iNPHRS total score).

Among the radiological measures, IIIvH was the only index that differed significantly between the two motor phenotypes, given higher values in patients with phenotype 2 (Figure 2).

3.2 Clinical correlations of MRI indexes

Correlation analyses between neuroimaging indices and clinical scores in the entire patients' cohort are detailed in Table 2, several of these were significant (*p*-values below 0.05). EI showed a negative correlation with the iNPHRS total score (including its gait and continence domains). We found a positive correlation of CA with the iNPHRS total score and its gait, balance and continence domains. By contrast, CA negatively correlated with the MDS-UPDRS III score. ALVI R/L showed a negative correlation with the iNPHRS total score and its gait and balance domains, while only ALVI L negatively correlated with the continence domain and only ALVI R positively correlated with the MDS-UPDRS III score. MRHI and both ALVI R/L were the only indices that negatively correlated with the MoCA score. We did not find any significant correlation of clinical scores with DESH, mCMI R/L, IIIvH, and IIIvLL. Nonetheless, IIIvH showed trends

of correlation with the severity of parkinsonism and urinary impairment (MDS-UPDRS III and iNPHRS continence scores, respectively) (Supplementary Figure 1).

Clinical-radiological correlations for each motor phenotype are reported in Supplementary Tables 1, 2 (phenotype 1 and phenotype 2, respectively). A negative correlation of EI with the iNPHRS total score (and its gait and continence domains) was confirmed only in the phenotype 1, where EI also showed a positive correlation with the MDS-UPDRS III score. A positive correlation of CA with the iNPHRS total score (and its balance and continence domains) was found in the phenotype 2. The negative correlation of MRHI with the MoCA score was found in the phenotype 2, where MRHI also negatively correlated with the iNPHRS balance score. Conversely, MRHI positively correlated with the MDS-UPDRS III score in the phenotype 1. The negative correlation of ALVI R/L with the iNPHRS total score (as well as its gait item) was shown in the phenotype 1, while ALVI R/L negatively correlated with the balance domain in the phenotype 2. Of note, ALVI R/L positively correlated with the MDS-UPDRS III score in both phenotypes. IIIvLL negatively correlated with the iNPHRS total score and positively correlated with the MDS-UPDRS III score in the phenotype 1. As in the entire cohort, we did not find any statistically significant correlation of clinical scores with DESH, mCMI R/L, and IIIvH for both phenotype 1 and 2.

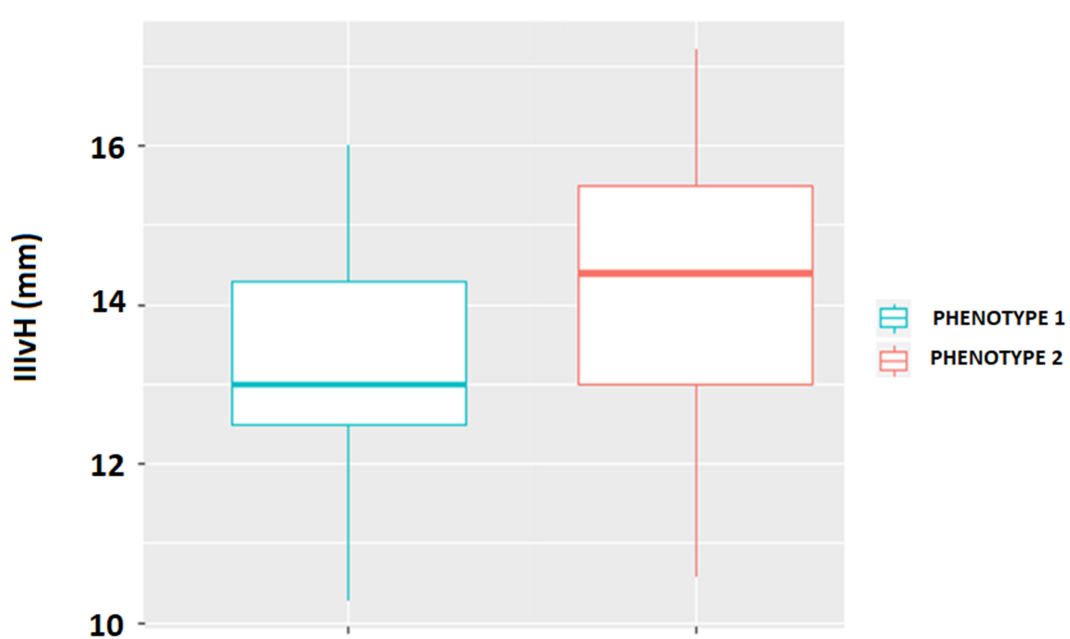


FIGURE 2 Comparison of the Height of the third ventricle between phenotype 1 (disequilibrium subtype) and phenotype 2 (parkinsonian subtype) of higher-level gait disorder. The difference was explored with the Wilcoxon test ($p = 0.017$).

TABLE 2 Correlations between radiological indices and clinical scores in the entire patients' cohort.

	MDS -UPDRS III	iNPHRS gait	iNPHRS balance	iNPHRS continence	iNPHRS total	MMSE	MoCA
EI	0.134	-0.250*	-0.198	-0.264*	-0.270*	-0.129	-0.229
CA	-0.0279*	0.359***	0.357***	0.288**	0.320**	0.102	0.106
DESH	482 (0.256)	652 (0.262)	615.5 (0.125)	657.5 (0.208)	640 (0.212)	376 (0.255)	349 (0.203)
MRHI	0.185	-0.188	-0.160	0.031	-0.0124	-0.212	-0.372**
ALVI R	0.009	-0.293**	-0.266*	-0.173	0.008	-0.232	-0.334**
ALVI L	0.087	-0.259*	-0.304**	-0.251*	0.008	-0.191	-0.297*
mCMI R	-0.039	0.058	-0.014	-0.0923	0.004	0.098	-0.048
mCMI L	-0.015	0.034	-0.135	0.065	-0.018	0.113	-0.106
IIIvH	0.203	-0.010	-0.113	-0.198	-0.115	0.199	0.177
IIIvLL	-0.069	0.060	-0.068	-0.133	-0.047	0.316	0.907

Statistical correlations between linear radiological features and clinical scales are assessed by Spearman correlation test, except for DESH by the Wilcoxon rank sum test with continuity correction with Cohen's d effect size in brackets. Statistically significance values are in bold. * p -value < 0.05; ** p -value < 0.01; *** p -value < 0.001. ALVI, Anteroposterior diameter of the Lateral Ventricle Index; CA, callosal angle; DESH, Disproportionately Enlarged Subarachnoid Space Hydrocephalus; EI, Evans' Index; iNPH, idiopathic normal pressure hydrocephalus; iNPHRS, iNPH Rating Scale; L, left; mCMI, modified Cella Media Index; MDS-UPDRS III, motor score of the Movement Disorder Society-Unified Parkinson's Disease Rating Scale; MMSE, Mini Mental State Examination; MoCA, Montreal Cognitive Assessment; MRHI, Magnetic Resonance Hydrocephalic Index; R, right; IIIvH, height of the third ventricle; IIIvLL, width of the third ventricle.

4 Discussion

In this study, we explored differences in eight linear MRI indexes and their clinical correlations between the two motor phenotypes of iNPH. IIIvH was the only neuroimaging feature that differed between the two motor phenotypes, being higher in iNPH patients with parkinsonian subtype of HLGD who showed also a greater global clinical impairment in terms of severity of motor, urinary and cognitive dysfunction, compared to subjects with disequilibrium subtype. It is also worth noting that, although not statistically significant, the clinical relevance of IIIvH may also

be supported by trends in correlation with overall parkinsonian and urinary symptom burden.

The pathophysiology of parkinsonian symptoms in hydrocephalic state is still unclear, probably multifactorial. It has been hypothesized that an increased IIIvH may cause a direct top-down compression on the rostral midbrain, resulting in a reduced mesencephalic volume. In iNPH patients, the midbrain diameter, in fact, was found to be decreased, showing an inverse correlation with the width of the third ventricle and the severity of gait disturbance (Lee et al., 2005). Alternatively, the midbrain compression deriving from a dilated third ventricle may cause a chronic deafferentation (Lee et al., 2005), leading a dysfunction of

neuronal groups of specific mesencephalic areas that are crucial for the control of gait and balance, such as the pedunculopontine nucleus, generating a phenotype similar to that observed in Parkinson's disease (Sébillé et al., 2019; Lee et al., 2000). The substantia nigra is another midbrain nucleus whose impairment may be involved in the pathophysiology of parkinsonism frequently observed in iNPH (Youn et al., 2022). Of note, density of striatal dopamine reuptake transporter was described to be abnormal in iNPH, and particularly lower in patients with parkinsonian subtype as compared to subjects with disequilibrium subtype of HLGD (Todisco et al., 2021; Pozzi et al., 2021). Furthermore, the impairment of the nigrostriatal dopaminergic function correlated with the severity of parkinsonism (Todisco et al., 2021; Pozzi et al., 2021). An alteration of the nigrostriatal system due to an expanding IIIv has been also suggested in some cases of different non-communicating forms of hydrocephalus and secondary parkinsonism as well, also due to aqueductal stenosis, as shown in the literature (Lee et al., 2005; Curran and Lang, 1994; Zeidler et al., 1998).

A midbrain dysfunction could contribute to impair urinary storage function in iNPH. The periaqueductal gray matter is a key mesencephalic area for micturition control, being connected both to upstream cortical and diencephalic centers (e.g., prefrontal, cingulate and insular cortex, thalamus and medial preoptic area of hypothalamus) and to downstream pontine and sacral spinal segments (e.g., Barrington's nucleus and Onuf's nucleus) that regulate bladder function (Zare et al., 2019). It has been suggested to be affected in iNPH, given the suggestion that a dysfunction of this midbrain area may contribute to determine small bladder capacity and detrusor overactivity observed in these patients (Sakakibara et al., 2008).

We found that a higher EI, a reduced CA, and a greater ALVI R/L were relevant radiological features associated with the severity of motor and urinary symptoms in our patients' cohort. Notably, CA was the single index showing the most significant values at correlation analyses with clinical scores, in keeping with other authors (Kockum et al., 2018), also considering its recently proved reliability in follow-up after shunt surgery, where an increase in CA was observed alongside neurologic improvement (Casimiro Reis et al., 2024). Considering that these linear radiological measures reflect morphology and volume of the lateral ventricles, it is reasonable to assume that the ventricular dilatation at this level can account for urinary dysfunction and multiple aspects of motor impairment, involving gait, balance, and appendicular movements possibly due to white matter disorders as detected by DTI technique (Marumoto et al., 2012). On a histological level, these patients present focal destruction of the ependyma with distortion and collapse of capillaries and chronic oedema or ischemic demyelination (Del Bigio, 1993), however, whether the ventricular dilatation is the *primum movens* or rather an epiphenomenon of an alternative pathophysiological mechanism remains to be demonstrated.

In parallel, we detected an increase of MRHI and ALVI R/L in association with the severity of cognitive decline, assessed by the MoCA score. These findings can emphasize the role of periventricular regions known to be involved in several associative cognitive functions, in particular corpus callosum and cingulum, indirectly measured by ALVI R/L, and arcuate fasciculus, indirectly measured by MRHI (Güngör et al., 2017; Lin et al., 2014). It could

be suggested that transependymal diffusion, oedema, and stretch or compression of these periventricular regions may be engaged in cognitive deficits of iNPH patients, as confirmed by a tractography study (Keong et al., 2017).

On the one hand, mCMI R/L and DESH did not disclose any correlation with the clinical scores. It could be argued that mCMI R/L is not as sensitive as other radiological indices in quantifying the extent of ventricular dilatation, while the qualitative observation of DESH in the majority of iNPH patients does not allow adequate investigation of the links to the multifaceted phenomenology of these patients. With this regard, the quantitative assessment of DESH could be desirable to improve the chance to detect clinical-radiological correlations. On the other hand, and differently from MoCA, MMSE score did not correlate with any radiological index. The report of high sensitivity, lack of ceiling effect, and good detection of cognitive heterogeneity could make MoCA a better measure of cognitive function as compared to MMSE (Jia et al., 2021), and thus potentially preferable to improve the cognitive characterization of iNPH patients and to effectively assess correlations with neuroimaging features.

The intra-group analyses showed that motor phenotypes were featured by different correlations of radiological indexes with clinical scores. In fact, EI, MRHI, and IIIvLL correlated with several motor and cognitive scores in patients with disequilibrium subtype, whereas MRHI was valuable measure in patients with parkinsonian subtype being correlated with balance impairment and cognitive severity. Instead, only ALVI R/L correlated with several motor scores in both gait subtypes. Once again, the peculiar radiological characterization of each motor phenotype of HLGD could be explained by distinct pathophysiological basis underlying the heterogenous phenomenological expression of iNPH.

The study has several limitations. Firstly, the small cohort of patients and the inhomogeneity of the sample due to the definite prevalence of the parkinsonian motor phenotype must be considered. Furthermore, due to the high number of correlations and the exploratory nature of the study, a multiple comparison was not feasible, although this model would have taken into account additional inter- and intra-individual clinical and anatomical variables that might influence these correlations.

Those linear radiological indices, even if more practical and applicable to CT images, may be less accurate than volumetric analysis, suggesting the need for further validation through brain 3D measurements as well. Although, our findings suggest the possible role of these neuroimaging markers in clinical practice for supporting diagnosis and for monitoring the clinical evolution of the disease, also over time. The radiological characterization of motor phenotypes of iNPH may benefit from further investigation using tractography or other advanced MRI imaging techniques i.e., functional MRI or multicompartamental diffusion model imaging to understand the underlying pathophysiology (Keong et al., 2017; Siasios et al., 2016).

Data availability statement

The datasets presented in this study can be found in online repositories. The names of the repository/repositories and accession number(s) can be found in this article/[Supplementary material](#).

Ethics statement

The study involving humans was approved by the Territorial Ethics Committee Lombardia 6. The study were conducted in accordance with the local legislation and institutional requirements. The participants provided their written informed consent to participate in this study.

Author contributions

SN: Conceptualization, Investigation, Writing – original draft, Writing – review and editing. MT: Conceptualization, Data curation, Funding acquisition, Investigation, Project administration, Resources, Writing – review and editing. MP: Conceptualization, Data curation, Investigation, Supervision, Writing – review and editing. EC: Supervision, Validation, Visualization, Writing – review and editing. FT: Data curation, Investigation, Methodology, Writing – review and editing. EB: Data curation, Formal Analysis, Writing – review and editing. FV: Supervision, Validation, Visualization, Writing – review and editing. RZ: Supervision, Validation, Visualization, Writing – review and editing. SF: Data curation, Formal Analysis, Writing – review and editing. GC: Supervision, Validation, Visualization, Writing – review and editing. CP: Supervision, Validation, Visualization, Writing – review and editing. AP: Supervision, Validation, Visualization, Writing – review and editing.

Funding

The authors declare that financial support was received for the research and/or publication of this article. This work was funded by RC 2025-2027, Italian Ministry of Health.

References

- Casimiro Reis, R., Harumi Gobbato Yamashita, R., Fontoura Solla, D., Fajardo Ramin, L., de Andrade Lourenção Freddi, T., Jacobsen Teixeira, M., et al. (2024). Changes in callosal angle and evans index after shunt surgery in patients with idiopathic normal pressure hydrocephalus. *World Neurosurg.* 190, e617–e621. doi: 10.1016/j.wneu.2024.07.191
- Cohen, J. (1992). A power primer. *Psychol. Bull.* 112, 155–159. doi: 10.1037//0033-2909.112.1.155
- Curran, T., and Lang, A. (1994). Parkinsonian syndromes associated with hydrocephalus: Case reports, a review of the literature, and pathophysiological hypotheses. *Mov. Disord.* 9, 508–520. doi: 10.1002/mds.870090503
- Del Bigio, M. (1993). Neuropathological changes caused by hydrocephalus. *Acta Neuropathol.* 85, 573–585. doi: 10.1007/BF00334666
- Goetz, C., Tilley, B., Shaftman, S., Stebbins, G., Fahn, S., Martinez-Martin, P., et al. (2008). Movement Disorder Society-sponsored revision of the Unified Parkinson's Disease Rating Scale (MDS-UPDRS): Scale presentation and clinimetric testing results. *Mov. Disord.* 23, 2129–2170. doi: 10.1002/mds.22340
- Güngör, A., Baydin, S., Middlebrooks, E., Tanriover, N., Isler, C., and Rhoton, A. (2017). The white matter tracts of the cerebrum in ventricular surgery and hydrocephalus. *J. Neurosurg.* 126, 945–971. doi: 10.3171/2016.1.JNS152082
- He, W., Fang, X., Wang, X., Gao, P., Gao, X., Zhou, X., et al. (2020). A new index for assessing cerebral ventricular volume in idiopathic normal-pressure hydrocephalus: A comparison with Evans' index. *Neuroradiology* 62, 661–667. doi: 10.1007/s00234-020-02361-8
- Hellström, P., Klinge, P., Tans, J., and Wikkelsø, C. (2012). A new scale for assessment of severity and outcome in iNPH. *Acta Neurol. Scand.* 126, 229–237. doi: 10.1111/j.1600-0404.2012.01677.x
- Ishii, K., Kanda, T., Harada, A., Miyamoto, N., Kawaguchi, T., Shimada, K., et al. (2008). Clinical impact of the callosal angle in the diagnosis of idiopathic normal pressure hydrocephalus. *Eur. Radiol.* 18, 2678–2683. doi: 10.1007/s00330-008-1044-4
- Jia, X., Wang, Z., Huang, F., Su, C., Du, W., Jiang, H., et al. (2021). A comparison of the Mini-Mental State Examination (MMSE) with the Montreal Cognitive Assessment (MoCA) for mild cognitive impairment screening in Chinese middle-aged and older population: A cross-sectional study. *BMC Psychiatry* 21:485. doi: 10.1186/s12888-021-03495-6
- Keong, N., Pena, A., Price, S., Czosnyka, M., Czosnyka, Z., DeVito, E., et al. (2017). Diffusion tensor imaging profiles reveal specific neural tract distortion in normal pressure hydrocephalus. *PLoS One* 12:e0181624. doi: 10.1371/journal.pone.0181624
- Kockum, K., Lilja-Lund, O., Larsson, E., Rosell, M., Söderström, L., Virhammar, J., et al. (2018). The idiopathic normal-pressure hydrocephalus Radscale: A radiological scale for structured evaluation. *Eur. J. Neurol.* 25, 569–576. doi: 10.1111/ene.13555
- Kojoukhova, M., Koivisto, A., Korhonen, R., Remes, A., Vanninen, R., Soininen, H., et al. (2015). Feasibility of radiological markers in idiopathic normal pressure hydrocephalus. *Acta Neurochir.* 157, 1709–18; discussion 1719. doi: 10.1007/s00701-015-2503-8
- Lee, M., Rinne, J., and Marsden, C. (2000). The pedunculo-pontine nucleus: Its role in the genesis of movement disorders. *Yonsei Med. J.* 41, 167–184. doi: 10.3349/ymj.2000.41.2.167

Conflict of interest

The authors declare that the research was conducted in the absence of any commercial or financial relationships that could be construed as a potential conflict of interest.

Generative AI statement

The authors declare that no Generative AI was used in the creation of this manuscript.

Publisher's note

All claims expressed in this article are solely those of the authors and do not necessarily represent those of their affiliated organizations, or those of the publisher, the editors and the reviewers. Any product that may be evaluated in this article, or claim that may be made by its manufacturer, is not guaranteed or endorsed by the publisher.

Supplementary material

The Supplementary Material for this article can be found online at: <https://www.frontiersin.org/articles/10.3389/fnagi.2025.1554642/full#supplementary-material>

- Lee, P., Yong, S., Ahn, Y., and Huh, K. (2005). Correlation of midbrain diameter and gait disturbance in patients with idiopathic normal pressure hydrocephalus. *J. Neurol.* 252, 958–963. doi: 10.1007/s00415-005-0791-2
- Lin, Y., Shih, Y., Tseng, W., Chu, Y., Wu, M., Chen, T., et al. (2014). Cingulum correlates of cognitive functions in patients with mild cognitive impairment and early Alzheimer's disease: A diffusion spectrum imaging study. *Brain Topogr.* 27, 393–402. doi: 10.1007/s10548-013-0346-2
- Marumoto, K., Koyama, T., Hosomi, M., Kodama, N., Miyake, H., and Domen, K. (2012). Diffusion tensor imaging in elderly patients with idiopathic normal pressure hydrocephalus or Parkinson's disease: Diagnosis of gait abnormalities. *Fluids Barriers CNS* 9:20. doi: 10.1186/2045-8118-9-20
- Nakajima, M., Yamada, S., Miyajima, M., Ishii, K., Kuriyama, N., Kazui, H., et al. (2021). Guidelines for management of idiopathic normal pressure hydrocephalus (Third Edition): Endorsed by the Japanese society of normal pressure hydrocephalus. *Neurol Med. Chir.* 61, 63–97. doi: 10.2176/nmc.st.2020-0292
- Nutt, J. (2013). Higher-level gait disorders: An open frontier. *Mov. Disord.* 28, 1560–1565. doi: 10.1002/mds.25673
- Pozzi, N., Brumberg, J., Todisco, M., Minafra, B., Zangaglia, R., Bossert, I., et al. (2021). Striatal dopamine deficit and motor impairment in idiopathic normal pressure hydrocephalus. *Mov. Disord.* 36, 124–132. doi: 10.1002/mds.28366
- Quattrone, A., Sarica, A., La Torre, D., Morelli, M., Vescio, B., Nigro, S., et al. (2020). Magnetic resonance imaging biomarkers distinguish normal pressure hydrocephalus from progressive supranuclear palsy. *Mov. Disord.* 35, 1406–1415. doi: 10.1002/mds.28087
- Reinard, K., Basheer, A., Phillips, S., Snyder, A., Agarwal, A., Jafari-Khouzani, K., et al. (2015). Simple and reproducible linear measurements to determine ventricular enlargement in adults. *Surg. Neurol. Int.* 6:59. doi: 10.4103/2152-7806.154777
- Relkin, N., Marmarou, A., Klinge, P., Bergsneider, M., and Black, P. (2005). Diagnosing idiopathic normal-pressure hydrocephalus. *Neurosurgery* 57(3 Suppl.), S4–S16. doi: 10.1227/01.neu.0000168185.29659.c5
- Sakakibara, R., Kanda, T., Sekido, T., Uchiyama, T., Awa, Y., Ito, T., et al. (2008). Mechanism of bladder dysfunction in idiopathic normal pressure hydrocephalus. *Neurol. Urodyn.* 27, 507–510. doi: 10.1002/nau.20547
- Sébille, S., Rolland, A., Faillot, M., Perez-Garcia, F., Colomb-Clerc, A., Lau, B., et al. (2019). Normal and pathological neuronal distribution of the human mesencephalic locomotor region. *Mov. Disord.* 34, 218–227. doi: 10.1002/mds.27578
- Siasios, I., Kapsalaki, E., Fountas, K., Fotiadou, A., Dorsch, A., Vakharia, K., et al. (2016). The role of diffusion tensor imaging and fractional anisotropy in the evaluation of patients with idiopathic normal pressure hydrocephalus: A literature review. *Neurosurg. Focus* 41:E12. doi: 10.3171/2016.6.FOCUS.06192
- Todisco, M., Picascia, M., Pisano, P., Zangaglia, R., Minafra, B., Vitali, P., et al. (2020). Lumboperitoneal shunt in idiopathic normal pressure hydrocephalus: A prospective controlled study. *J. Neurol.* 267, 2556–2566. doi: 10.1007/s00415-020-09844-x
- Todisco, M., Pozzi, N., Zangaglia, R., Minafra, B., Servello, D., Ceravolo, R., et al. (2019). Pisa syndrome in idiopathic normal pressure hydrocephalus. *Parkinsonism Relat. Disord.* 66, 40–44. doi: 10.1016/j.parkreldis.2019.06.024
- Todisco, M., Valentino, F., Alfonsi, E., and Cosentino, G. (2022). Camptocormia in idiopathic normal pressure hydrocephalus: A case report. *Acta Neurol. Belg.* 122, 1127–1129. doi: 10.1007/s13760-021-01666-6
- Todisco, M., Zangaglia, R., Minafra, B., Pisano, P., Trifirò, G., Bossert, I., et al. (2021). Clinical outcome and striatal dopaminergic function after shunt surgery in patients with idiopathic normal pressure hydrocephalus. *Neurology* 96, e2861–e2873. doi: 10.1212/WNL.0000000000012064
- Youn, J., Todisco, M., Zappia, M., Pacchetti, C., and Fasano, A. (2022). Parkinsonism and cerebrospinal fluid disorders. *J. Neurol. Sci.* 433:120019. doi: 10.1016/j.jns.2021.120019
- Zare, A., Jahanshahi, A., Rahnama'i, M., Schipper, S., and van Koeveeringe, G. (2019). The role of the periaqueductal gray matter in lower urinary tract function. *Mol. Neurobiol.* 56, 920–934. doi: 10.1007/s12035-018-1131-8
- Zeidler, M., Dorman, P., Ferguson, I., and Bateman, D. (1998). Parkinsonism associated with obstructive hydrocephalus due to idiopathic aqueductal stenosis. *J. Neurol. Neurosurg. Psychiatry* 64, 657–659. doi: 10.1136/jnnp.64.5.657